Cytotechnology (2018) 70:13–29
https://doi.org/10.1007/s10616-017-0168-2

METHODS PAPER

Comparison of biophysical properties characterized for microtissues cultured using microencapsulation and liquid crystal based 3D cell culture techniques

Chin Fhong Soon · Kian Sek Tee · Soon Chuan Wong · Nafarizal Nayan · Sargunan Sundra · Mohd Khairul Ahmad · Farshid Sefat · Naznin Sultana · Mansour Youseffi

Received: 20 April 2017 / Accepted: 9 November 2017 / Published online: 30 November 2017

Abstract Growing three dimensional (3D) cells is an emerging research in tissue engineering. Biophysical properties of the 3D cells regulate the cells growth, drug diffusion dynamics and gene expressions. Scaffold based or scaffoldless techniques for 3D cell cultures are rarely being compared in terms of the physical features of the microtissues produced. The biophysical properties of the microtissues cultured using scaffold based microencapsulation by flicking and scaffoldless liquid crystal (LC) based techniques were characterized. Flicking technique produced high yield and highly reproducible microtissues of keratinocyte cell lines in alginate microcapsules at approximately 350 ± 12 pieces per culture. However, microtissues grown on the LC substrates yielded at lower quantity of 58 ± 21 pieces per culture. The sizes of the microtissues produced using alginate microcapsules and LC substrates were 250 ± 25 μm and 141 ± 70 μm, respectively. In both techniques, cells remodeled into microtissues via different growth phases and showed good integrity of cells in field-emission scanning microscopy (FE-SEM). Microencapsulation packed the cells in alginate scaffolds of polysaccharides with limited spaces for motility. Whereas, LC substrates allowed the cells to migrate and self-stacking into multilayered structures as revealed by the nuclei stainings. The cells cultured using both techniques were found viable based on the live and dead cell stainings. Stained histological sections showed that both techniques produced cell models that closely replicate the intrinsic physiological conditions. Alginate microcapsulation and LC based techniques produced microtissues containing similar bio-macromolecules but they did not alter the main absorption bands of microtissues as revealed by the Fourier transform infrared spectroscopy. Cell growth, structural organization, morphology and surface structures for 3D microtissues cultured using both techniques appeared to be different and might be suitable for different applications.

Keywords 3D cell culture · Biophysical properties · Liquid crystal · Microtissues · Keratinocytes · Microencapsulation

C. F. Soon (✉) · K. S. Tee · S. C. Wong · N. Nayan · Sargunan Sundra · M. K. Ahmad
Biosensor and Bioengineering Lab, MiNT-SRC, Faculty of Electrical and Electronic Engineering, Universiti Tun Hussein Onn Malaysia, 86400 Parit Raja, Batu Pahat, Johor, Malaysia
e-mail: soon@uthm.edu.my

N. Sultana
Faculty of Biosciences and Medical Engineering, Universiti Teknologi Malaysia, 81310 Skudai, Johor, Malaysia

F. Sefat · M. Youseffi
Faculty of Engineering and Informatics, Medical and Healthcare Technology Department, University of Bradford, Bradford BD7 1DP, UK

Introduction

Sub-culturing monolayer of cells in plastic vessels is a routine procedure for cell biology studies. However, the reliability of using 2D or monolayer cell model for cell biology or pharmacological studies is controversial (Antoni et al. 2015). Cells grown in monolayer proliferate involuntarily due to the contactless spreading of cells and it has been shown to produce limited secretion of extracellular matrix (ECM) proteins (Souza et al. 2010; Yamada and Cukierman 2007). The cells proliferation, differentiation, morphology, protein expressions and general cell function are considerably different from their physiological origin in vivo (Edmondson et al. 2014). In contrast, 3D cell culture creates an artificial environment in which, biological cells can grow and interact with the surrounding environment in three dimensions. 3D cell culture systems are believed to have better approximation to the in vivo system (Antoni et al. 2015; Edmondson et al. 2014) because it reconstructs specific biochemical and morphological features similar to the tissue in vivo. The connections between cells are more native-like and hence, 3D cell culture technique is a promising approach in bridging 2D cell model and animal model.

Although not widely spread, 3D cell cultures are beginning to gain recognitions as more physiologically relevant models because 3D cell models improve the prediction of drug development process (Fang and Elgen 2017; Hirschhaeuser et al. 2010; Kunz-Schughart et al. 2014). Some popular approaches for culturing 3D cells are such as hanging drops, micromolded agarose gel, planar matrix, scaffolds of hydrogels and bioreactor based methods (Nirmalanandhan et al. 2010; Vantangoli et al. 2015). These techniques are divided into scaffold based and scaffoldless 3D cell culture techniques. Scaffold based method can be constructed from polymeric materials that are designed to mimic the in vivo ECM of the specific tissues with different porosities, permeability and mechanical characteristics (Antoni et al. 2015). Usually, cells grow in the porous structures of the scaffolds. On the other hand, 3D cell culture based on scaffold-free planar matrix do not require additional biomolecules or ECM proteins. Cells are able to be grown and organized using self-derived ECM proteins on the planar matrix (Hirschhaeuser et al. 2010). Scaffoldless culture technique based on hydrogel (agarose, collagen and alginate) aim to mimic the ECM while providing high compliant substrates for the cells to grow into microtissues (Wong et al. 2016). Hanging drop method is another example of scaffoldless technique which can grow 3D cells in suspension of culture medium (Thoma et al. 2013).

However, techniques for culturing 3D cells in scaffold based or scaffold-free settings are being developed independently for different applications (Therese Andersen and Dornish 2015; Wang et al. 2009). There are lacking reports on investigating the structural organization, morphology and proliferation of cells in the microtissues formed using different 3D culture techniques (Edmondson et al. 2014). As revealed previously (Edmondson et al. 2014), the cancer cell lines can be organized into 3D spheroids of grape-like, mass, stellate and round structures. A previous study (Luca et al. 2013) indicated that colorectal cancer cell lines derived from metastatic cells induce grape-like morphology, however, the same cell lines from primary tumour tissue formed mass spheroid morphology. Nonetheless, the cellular morphological appearance of 3D spheroids are both found to be cell lines and culture systems dependent (Hongisto et al. 2013). Hence, different 3D culture systems are rarely being compared experimentally to understand the biophysical differences of the microtissues produced for similar or different cell types. The study of biophysical properties of the 3D spheroids is essential because the biophysical properties of 3D spheroids can influence the signal transduction from outside to the inside of cells, gene expression and cellular behaviors (Antoni et al. 2015).

In our lab, we have developed a novel microencapsulation technique based on flicking (Wong et al. 2016) and liquid crystal substrate to grow microtissues (Soon et al. 2016). Microencapsulation is a technology of packaging cells within alginate spheres (microcapsules) in single core or polycores. Flicking can be performed by tapping the extrusion of alginate solution from a syringe and breaking the alginate droplets into smaller size microcapsules. The objective of this paper is to identify the biophysical differences of microtissues generated from scaffold based flicking microencapsulation and scaffoldless liquid crystal substrate techniques. The study involved comparisons of two different 3D cell culture systems in influencing the growth phases, viability, surface morphology, biochemistry, nuclei organization and membrane structure for the same cell type.

Materials and methods

Cells preparation

Human keratinocyte (HaCaT) cell lines were purchased from Cell Line Services (CLS, Eppelheim, Germany) and maintained in a 25 cm^2 tissue-treated culture flasks containing Dulbecco's Modified Eagle Medium (DMEM, Gibco®, Life Technologies, Camarillo, CA, USA) culture medium. The DMEM medium was supplemented with 10% fetal bovine serum (FBS, Invitrogen, Carlsbad, CA, USA), penicillin (100 units/ml, Sigma Aldrich, Gillingham, UK), fungizone (2.5 mg/l, Sigma Aldrich) and streptomycin (100 µg/ml, Sigma Aldrich). The cells were incubated in a 5% CO_2 humidified environment at 37 °C. Upon reaching 80% confluency, the medium was removed from the flask and the flask was washed three times with Hank's Balanced Salt Solution (HBSS, Invitrogen). After removing the HBSS solution, 1 ml of 0.25% ethylenediamine-tetra-acetic acid (EDTA) crude trypsin (0.5 mg/ml, Sigma Aldrich) was put into the flask for approximately 5 min to detach the cells from the flask. Subsequently, 5 ml of DMEM containing FBS was put to the flask. The cell suspensions were then collected in a 15 ml tube and centrifuged at 1200 rpm for 5 min. When this process was completed, the supernatant was discarded and the cells were ready for the following experiment.

3D cell culture on liquid crystal substrate

A mixture of solid crystals of cholesteryl ester liquid crystal was melted at 110 °C (Soon et al. 2013) and 20 µl of the liquid crystal in isotropic phase was immediately transferred to a petri dish. The liquid crystal was squeegee coated using a squeegee coater and allowed to be cooled to room temperature. Alternatively, the liquid crystal can be coated on the dish surface using a cell scrapper in replacement of the squeegee coater. 1 ml of cells at a density of 5.5×10^5 cells/ml was deposited on the surface of the liquid crystal substrate followed by addition of 5 ml of DMEM culture media supplemented with nutrients. The cells were then incubated in an incubator (5% CO_2, 37 °C). After 5 days of incubation, the aggregates of cells formed into microtissues were removed from the medium and used for the characterization experiment.

Microencapsulation of 3D cells

The HaCaT cells contained in a 2 ml tube was supplemented with 100 µl of 1.5% w/v alginate solution at a cell density of 3×10^7 cells/ml. The cell-alginate suspensions were filled in a 0.5 ml syringe (Becton, Dickinson and Company, Franklin Lakes, NJ, USA) with a 29-gauge insulin needle and the syringe was fitted to a customized syringe pump functions to extrude the cells-alginate suspension. While the syringe pump was extruding the alginate/cells solution at a flow rate of 5 µl/min, the needle of syringe pump was simultaneously flicked at 80 rpm using a motorized flicking device. The fine droplets of alginate/cells dropped into a petri dish containing 4 ml of filtered calcium chloride solution and led to polymerization of the droplets into microcapsules containing the cells. The development of the flicker machine was as reported in Wong et al. (2016). Subsequently, the microencapsulated cells were removed from the chloride solution and incubated in 6 ml of DMEM medium at 37 °C. After 15 days of culture, the membrane of alginate encapsulating the microtissues was removed using 0.2 mg/ml of alginate lyase (A1603-100MG, Sigma Aldrich, St. Louis, MO, USA) and the microtissues were washed in HBSS. After alginate lyase treatment, the microtissue samples were ready for the biophysical characterization experiments.

Microscopy monitoring and image processing

The physical changes of the cells were observed every 24 h in an inverted phase contrast microscope (Nikon Eclipse TS-100, Tokyo, Japan) connected with a Go-3 charged coupled device (CCD) camera. The photomicrographs of the cell aggregates were captured using a QCapture Pro 6.0 software. By maintaining the brightness of the microscope, the cell density of microtissues formed using both culture techniques were indicated by the changes of gray level in the phase contrast photomicrographs captured. To compute the gray level (mean ± SD) of the microtissue which appeared in the phase contrast micrographs, the ImageJ (Version 1.51, National Institutes of Health, Bethesda, MD, USA) software was used. The images of microtissues in 24-bit colors were converted to 8-bit gray level images. Subsequently, the region of interest (ROI) of the microtissues were selected and the gray

level statistics of the ROI was computed using the histogram tool available in the ImageJ software. The gray level varying from black to white was mapped to 0–255 of gray scales, respectively. The gray levels of the images of the microtissues grown in alginate microcapsules and liquid crystal surfaces over 30 and 15 days, respectively, were computed and plotted.

For quantifying the size of the microtissues in microencapsulation (3D spheroids), the volume of the microtissues were calculated by using $V = \frac{4}{3}\pi r^3$, where r is the radius of the microspheroids. The gray level profile of the ROI of the microtissues is associated with the cell packing density and growth phases of the microspheroids.

Biophysical characterization of microtissues

FE-SEM imaging of the 3D microtissues

The 3D microtissues extracted from microcapsules and liquid crystal surfaces were fixed at 4% formaldehyde (Sigma Aldrich) solution for 24 h at 5 °C and followed by serial alcohol dehydration at 25, 50, 75 and 100% of ethanol. The dehydrated microtissues were placed on a glass slide and sputtered with conductive gold coatings in a JFC-1600 Auto Fine Coater (JEOL, Tokyo, Japan) powered at 20 mA for 30 s. Then, the glass slide was mounted to a mounting stub with a double-sided carbon tape and imaged in the FE-SEM. The microtissues were examined using a JSM-7600F field emission-scanning electron microscope (FE-SEM, JOEL) with an upper secondary electron imaging (SEI) detector. The samples were exposed to an accelerated voltage beam of 5 kV and the images were taken at 150 ×, 300 × and 10,000 × magnifications. The FE-SEM scanning of different samples was repeated for three times.

DAPI (4′, 6-diamidino-2-phenylindole dihydrochloride) staining

DAPI (4′, 6-diamidino-2-phenylindole dihydrochloride) stains the nucleus of the cells and this staining was used to identify the cell distribution in the microtissues formed. The microtissues was incubated in 0.1 μg/ml DAPI (Sigma Aldrich, St. Louis, MO, USA) diluted in HBSS for 20 min in dark. Subsequently, the DAPI stain solution was removed and the stained microtissues were washed three times with HBSS solution. The stained microtissue images were examined and captured in a BX53 fluorescence microscope (Olympus, Tokyo, Japan) mounted with a DP73 CCD camera (Olympus, Tokyo, Japan). Similar experiments were repeated for three times.

Live and dead cell staining

The viability of the cells in the microtissues cultured using the alginate microencapsulation and liquid crystal techniques were investigated using live/dead® viability kit for mammalian cells (Invitrogen, Paisley, UK). The live/dead® viability kit containing calcein-AM (20 μl, 2 mM in 10 ml HBSS) and ethidium homodimer-1 (EthD-1, 5 μl, 4 mM in 10 ml HBSS) reagents were prepared. The live/dead® cell viability kit can differentiate live cells from the dead cells by double staining the cells with green-fluorescent calcein-AM (Invitrogen) which indicates intracellular esterase activity, while, red-fluorescent ethidium homodimer-1 (EthD-1) (Invitrogen) indicates loss of plasma membrane integrity. Soon after removing the microtissues from the alginate microcapsules or liquid crystal substrates, the microtissues were incubated in 2 μM calcein-AM and 4 μM EthD-1 staining solutions for 20 min in the dark. The stained microtissues were captured using a BX53 fluorescence microscope (Olympus, Tokyo, Japan) mounted with a DP73 CCD camera. The live and dead experiments for the microtissues were repeated for three times.

Fourier transform infrared (FTIR) spectroscopy measurement

A FTIR spectrometer (Perkin Elmer Spectrum 100, Shelton, CT, USA) was used to perform Fourier transform infrared (FTIR) spectroscopy for the microtissues harvested from alginate microcapsules (after alginate lyase treatment) and liquid crystal cultures. Both samples were removed from the medium and placed on the window of the small-attenuated total reflection (ATR) crystal in the spectrometer. Then, the pressure arm was placed over the tissue sample. Perkin Elmer Spectrum Express software was used to acquire the infrared spectra of each sample using a scan rate of 32 scans per second at a spectral resolution of 4.0 cm^{-1}. The FTIR spectra were plotted over a spectral

range of 4000–600 cm^{-1}. Similar measurements were repeated for three times.

Histological sectioning and staining

The microtissues produced by liquid crystals and alginate microencapsulation techniques were removed from the cultures using a pair of tweezers. The microtissues of approximately 10 pieces from each culture were washed, fixed in 4% formaldehyde containing a few drops of eosin in a 2 ml polypropylene tube overnight at 5 °C. After fixation, the microtissues were removed from the formaldehyde and incubated in 70% ethanol for 3 h. Then, the microtissues were left air dried in two similar metal base molds. Paraffin pellets were heated in a pan at 100 °C in an oven and poured into the metal base molds containing the microtissues. The molds containing the tissues and liquid paraffin were each topped with a multi-cassette and left to cool at room temperature (25 °C). When the liquid paraffin was solidified, the blocks of paraffin and the cassettes in the mold were placed in a freezer at 0 °C. After 24 h, the block of paraffin was removed and placed in a Accu-Cut SRM 200 rotary microtome (Sakura Finetek Europe, Alphen aan den Rijn, Netherlands) for tissue sectioning at 5 μm of thickness. The sections of microtissues were collected on glass slides. Hematoxylin and Eosin (H and E) stainings of the microtissues were initiated with immersion of microtissues in 5 μl of 70% ethanol for 30 s on glass slides, followed by a wash in distilled water. The sections were stained in 5 μl of Mayer's hematoxylin for 1 min. Subsequently, the sections were rinsed carefully with distilled water and stained with 5 μl of eosin for 30 s. After staining, the sections were serially dehydrated in 70, 95 and 100% of alcohol. The samples were immersed with xylene for 2 min, then mounted in DPX mounting medium (Sigma Aldrich). The stained sections were observed in an inverted phase contrast microscope (Nikon Eclipse TS-100, Tokyo, Japan) connected with a Go-3 charged coupled device (CCD) camera. Similar experiments were repeated for three times.

Statistical analysis

The quantification of size (length of the microtissues) and number of microtissues were repeated for three times (N = 3). For each repeat of experiments, 45 and 376 pieces of microtissues were randomly selected from liquid crystal and alginate microencapsulation cultures, respectively. Then, the size of microtissues was determined. The data were expressed in mean ± standard deviation (SD). The normality test was performed on the size of microtissues measured for both techniques using the Kolmogorov–Smirnov test (significantly normal for $p \geq 0.05$) before student t test was applied for determining the significant differences in means using the Statistical Package for Social Sciences (SPSS, version 17) software. No statistical significant differences in the size of microtissues for both culture techniques (N = 3) was assumed in the Student t test. The comparison of means for $p \leq 0.05$ was considered statistical significant different.

Results

The size of the microtissues cultured on the liquid crystal substrates was relatively smaller (141 ± 70 μm) and significantly different ($p = 0$, $p < 0.05$, N = 3) from the microtissues formed using alginate microcapsules (250 ± 25 μm) as indicated in Fig. 1a. High variability of microtissue sizes ranging from (50 to 380 μm) was observed (Fig. 1b) using the liquid crystal based 3D cell culture or scaffoldless technique. In liquid crystal culture, the microtissues were formed by self-organization and hence, the size of the microtissues was uncontrollable. Comparatively, the size of microtissues shaped by microencapsulation was well regulated with lower variability ranging from 180 to 320 μm as shown in Fig. 1c.

In addition to the size, flicking microencapsulation technique (scaffold based technique) presented an advantage in producing high yield and a controllable quantity of microcapsules (350 ± 12). The spherical microtissues quantified on the liquid crystal substrate per culture was much reduced at 58 ± 21 spheroids and the reproducibility of similar quantity was also lower compared with the flicking technique. The microspheroids cultured on the liquid crystal substrates were prone to merge and formed large masses of microtissues greater than 500 μm in length, and thus, producing lesser microspheroids.

In-vitro growth of 3D cells into microtissues in alginate scaffolds took 15 days in comparison to 5 days for microtissues to develop on the scaffoldless

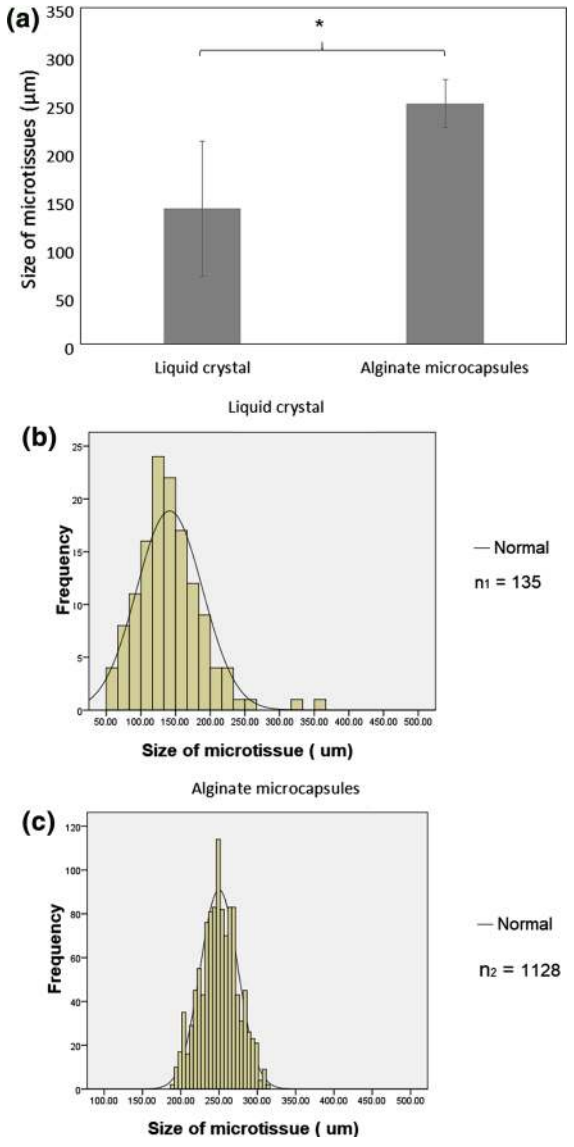

Fig. 1 **a** Size in mean ± SD ($p = 0$, $N = 3$) and **b**, **c** size distribution of microtissues produced using liquid crystal substrates and alginate microcapsules 3D cell culture techniques. *Indicates statistical significant difference for $p < 0.05$ as computed using Student's t test. Both data sets are normally distributed for liquid crystal and alginate microencapsulation based 3D cell cultures at $p = 0.2$ and $p = 0.07$, respectively (normal for $p > 0.05$, Kolmogorov-Smirnov test). The parameters, n_1 and n_2 are the total quantity of microtissues obtained from liquid crystal and alginate microencapsulation cultures for three repeats of experiments

liquid crystal substrate. In microencapsulation, the cells were restrained in proximity with great limitation of mobility within the alginate capsules while floating in the culture medium (Fig. 2a). In suspension culture format as shown in Fig. 2a, the cells took longer time to grow and form aggregates under buoyancy (unstable) condition with self secreted ECM (Fig. 2a). Although the microtissues seemed to be in spherical shape conforming to the shape of the alginate microcapsule (Fig. 2a), these microtissues were found to be in tortuous and spherical shape once removed from the alginate membrane as shown in Fig. 2b. In contrast, cells that were distributed on a stable liquid crystal substrate use their mechanotransducer to communicate with the adjacent cells and self-piling into microtissues (Fig. 2c). The microtissues formed by self-organization via migration on the liquid crystal substrates were well organized either in semi-spherical or elliptical shape.

Figure 3a shows the growth of the microtissues on the liquid crystal over 30 days of culture (N = 3). After 1 day of culture on the liquid crystal substrate, aggregates of cells in clusters began to develop on the liquid crystal substrates. The aggregates of cells continued to assemble into microtissues with higher cell density at a fixed location. This was indicated by the lower light penetration through the microtissues. After 5 days of culture on liquid crystal substrates, the microtissues with higher cell density appeared darken which seemed to be associated with the microtissues covered area (Fig. 3c). The cell density of the microtissues continued to increase (a decrease of gray level or darken) to a threshold on day 7 of culture and experienced small changes thereafter. Similarly, the area covered by microtissues increased to a peak on day 5 and decreased gradually over 30 days of culture (Fig. 3c). As shown in Fig. 3b, different growth phases such as lag, exponential, stationary and declining phases could be identified from gray level changes of the inverted phase contrast photomicrographs of microtissues.

Figure 4a shows the mapping of growth phases to the gray level of the encapsulated microspheroids. The transformation of individual bright and shiny cells into densely knitted cells of microspheroids can be observed. The gray level changes of the photomicrographs of the microspheroids are as shown in Fig. 4b. The decreased gray level representing the development from individual cells in capsules (day 1) into microtissues over 15 days of culture. This is probably attributed to the remodeling of self-secreted extracellular matrix proteins by the cells (Kundu et al. 2009). Dark masses of cells representing the remodeling of

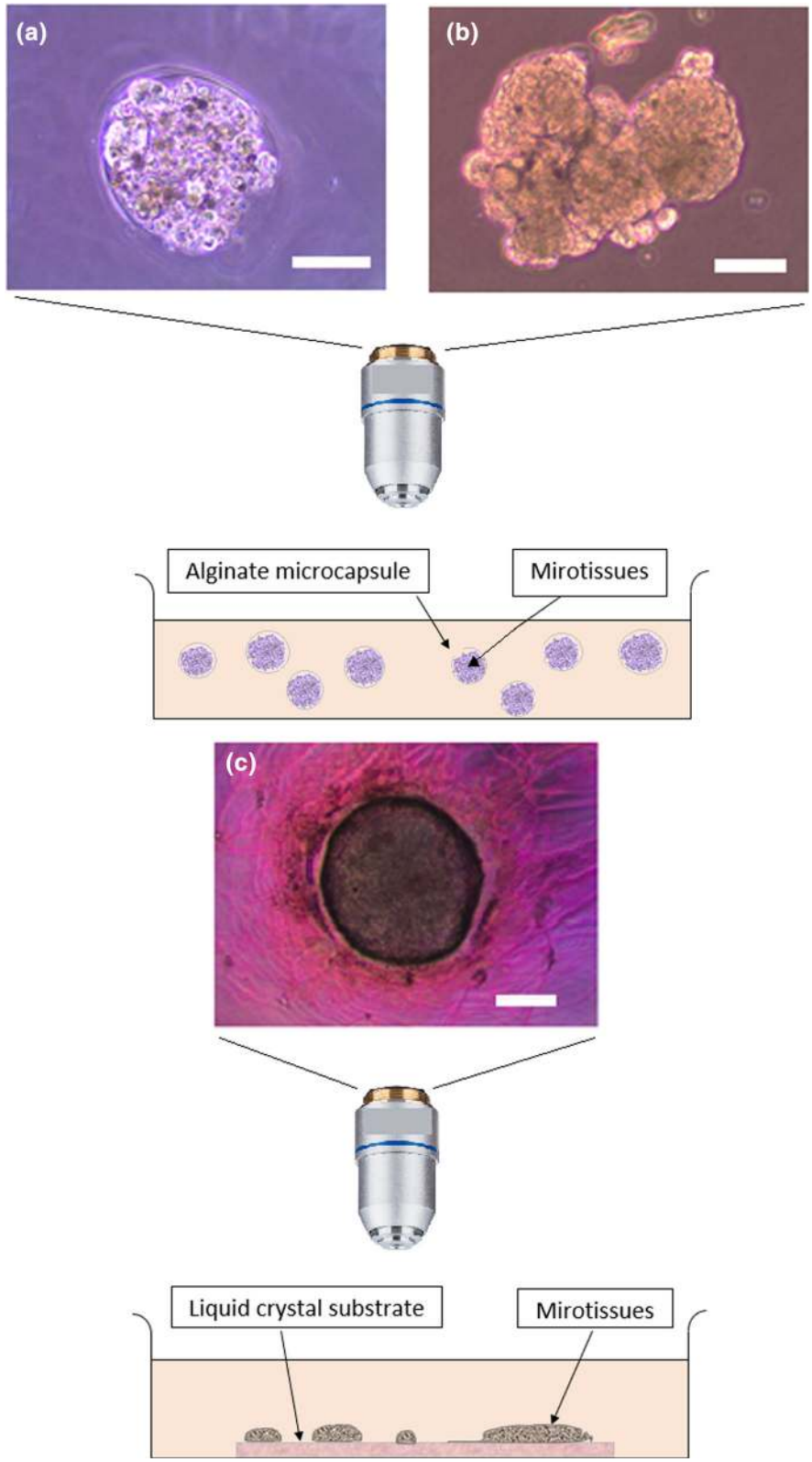

Fig. 2 The phase contrast photomicrographs and depictions of **a** 3D cells cultured in an alginate microcapsule suspended in culture medium, **b** the microtissues after alginate lyase treatment, and **c** microspheroids cultured on a liquid crystal substrate (scale bar: 100 μm)

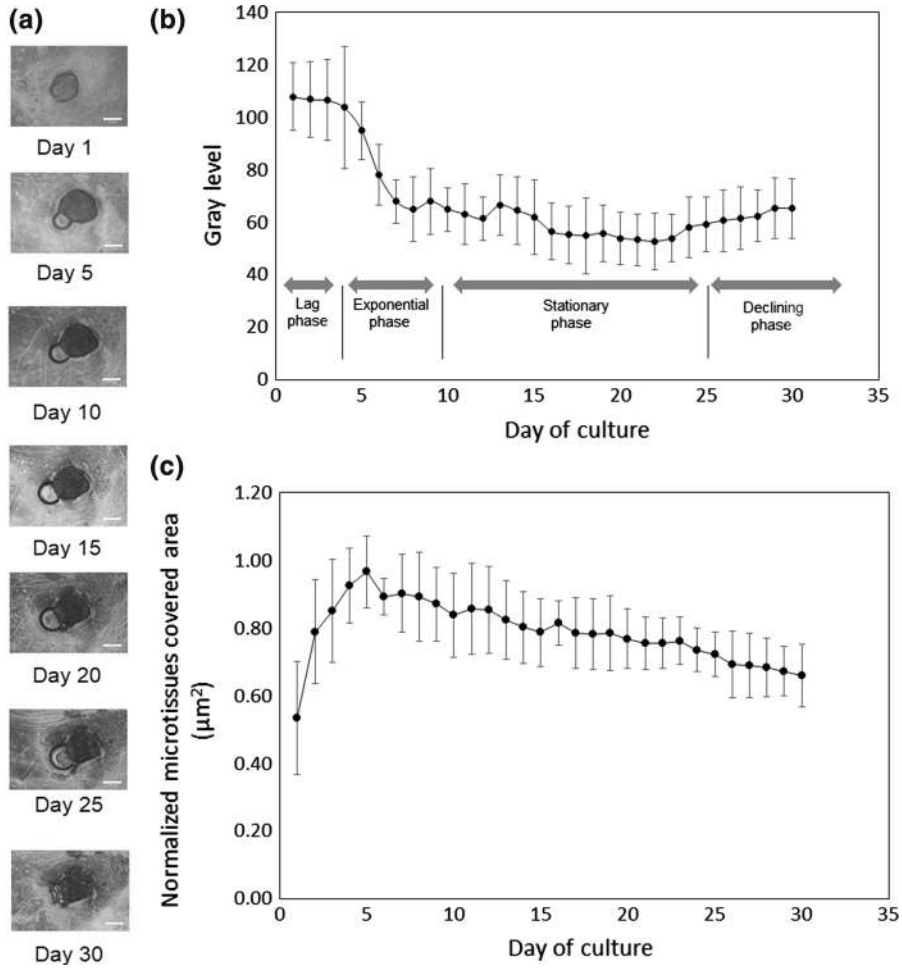

Fig. 3 **a** The phase contrast photomicrographs of microspheroids cultured on a liquid crystal in gray levels, **b** gray levels graph of microtissues images in mean ± SD and, **c** normalized microtissues covered area in μm^2 over a period of 30 days (scale bar: 100 μm)

cells initiated from the center core of the microtissues in microcapsules (Fig. 4a). The cells at the outer layer of the microtissues stayed shiny and bright in Fig. 4a. Similar to liquid crystal 3D cell culture technique, the lag, log and stationary phases can be identified. The declining phase occurred when the alginate membrane bursted and the cells leaked. Figure 4c shows that the microtissues in the capsules increased in volume and the volumetric growth turn stationary after approximately 5 days of culture.

The remodeling of cells into microtissues for both techniques were confirmed by FE-SEM. As seen in FE-SEM images (Fig. 5), the surface structures of the fixed microtissues formed using alginate microcapsules (Fig. 5a) and liquid crystal substrates (Fig. 5c) revealed strong cell–cell adhesion via the extracellular matrix proteins. Due to the alginate encapsulation, the surface structure of microtissues obtained from the alginate were more homogenous (Fig. 5b). Whereas microtissues extracted from the liquid crystal substrate were found having single cells protruding the surface of the microtissues (Fig. 5d). This is strongly associated with the unrestrained space for the cells growing in the culture medium.

Via the nuclei stainings (Fig. 6a, b), great differences in the arrangement of cells in the microtissues grown using both techniques were observed. Cells entrapped in the alginate membrane were randomly dispersed in the microencapsulation (Fig. 6a) at high cell packing density with a few apopotic cells residing in the center core of the microtissues. In contrast, the microtissues grown on liquid crystal surface were found to be arranged in stratified layers due to self-assembly and self-stacking to form multilayer structures (Fig. 6b). The microtissues grown using microcapsules (Fig. 6c) and liquid crystal substrate

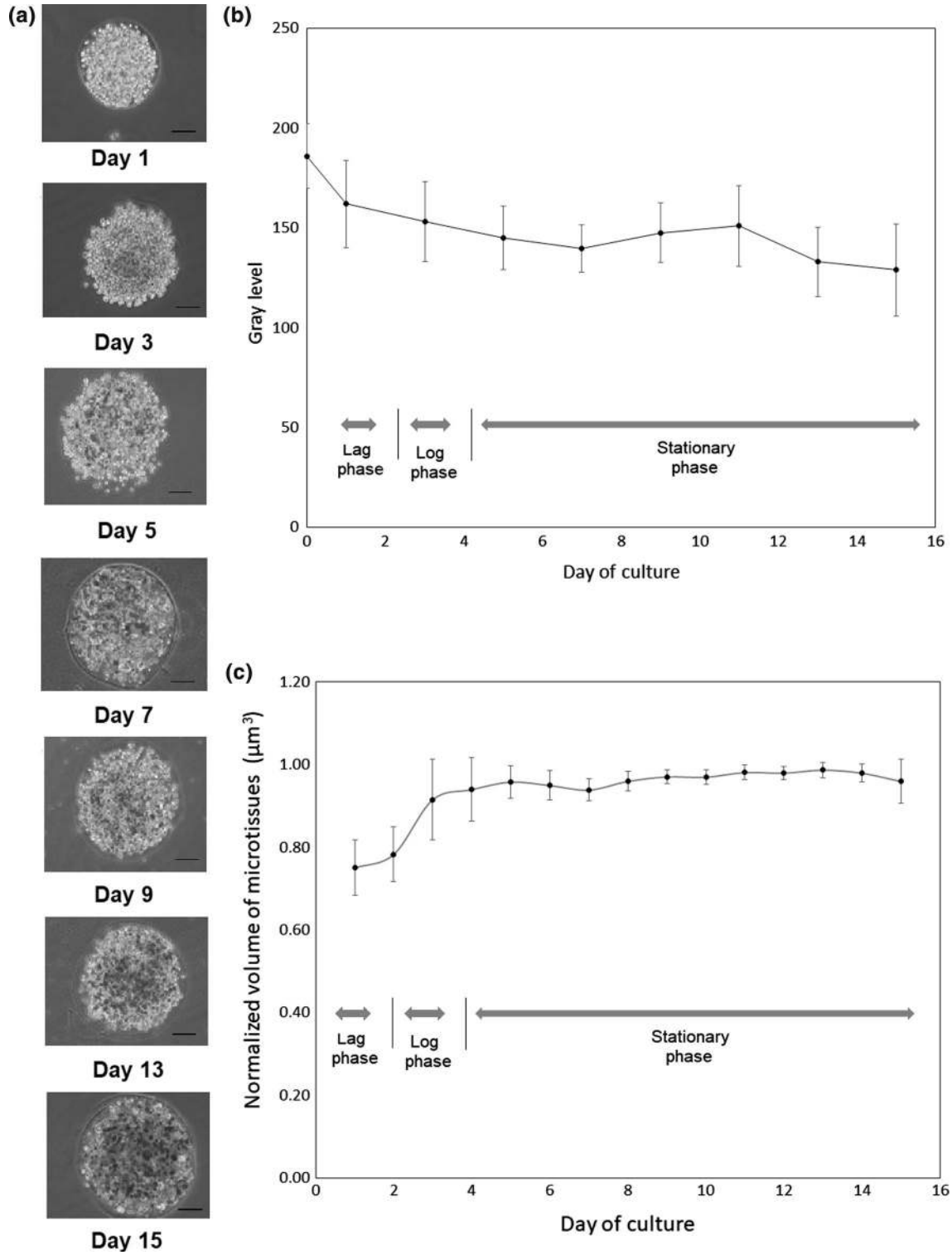

Fig. 4 **a** Phase contrast photomicrographs of microspheroids cultured in a alginate microcapsule in gray levels, **b** gray level of microtissues images in mean ± SD and, **c** normalized volume of microtissues in μm^3 over a period of 15 days (scale bar: 100 μm)

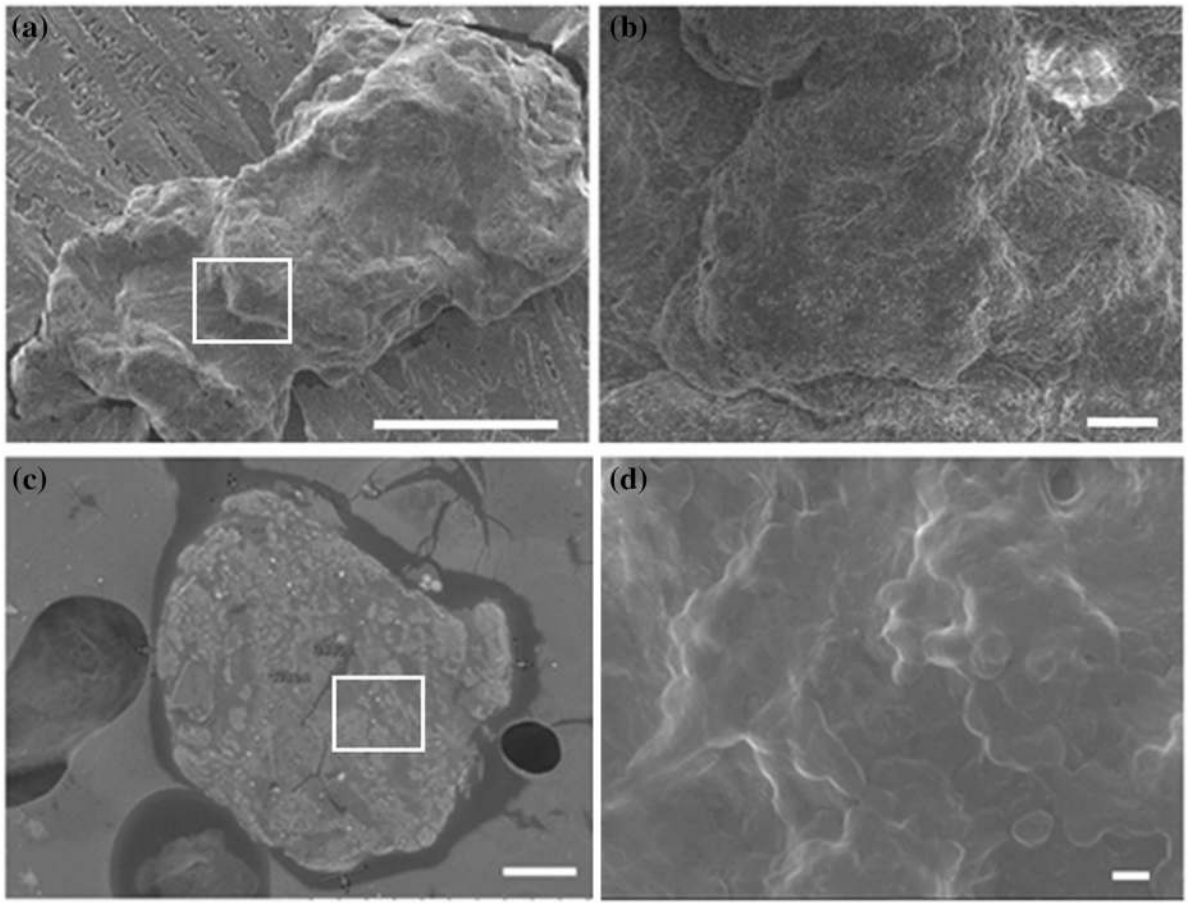

Fig. 5 FE-SEM photomicrographs of microtissues produced using **a** alginate microencapsulation (scale bar: 100 μm), **b** enlarged surface structure of (**a**) as indicated with a rectangle (scale bar: 10 μm), **c** liquid crystal substrate techniques (scale bar: 100 μm), and **d** enlarged surface structure of (**c**) as indicated with a rectangle (scale bar: 10 μm)

(Fig. 6d) techniques were characterized by highly viable cells with very few dead cells after 5 days of culture, respectively.

For the microtissues grown on the liquid crystal substrates, the absorption band at 3307 cm^{-1} was attributed to the symmetric O–H stretching (Fig. 7a). The two absorption bands at 2925 and 2852 cm^{-1} were attributed to the CH_2 asymmetric and symmetric stretches in lipids, respectively (Malek et al. 2014). The presence of Amide I and II proteins in the microtissues were attributed to the band of 1635 and 1550 cm^{-1}, respectively. Consequently, the absorption bands of the two amide groups characterized the proteins absorptions of the microtissues. The ionized asymmetry stretching of PO_2^- exhibits absorptions at 1290 and 1034 cm^{-1} that was attributed to the presence of nucleic acid (Jackson and Mantsch 1995) in the microtissues. The FTIR absorption spectra of the microtissue cultured on the liquid crystal showed different distribution of absorption bands from liquid crystal (Fig. 7a). For the spectra of the liquid crystal, two strong dips found at 2925 and 2850 cm^{-1} are similar to the absorption bands of the microtissues extracted from liquid crystal surface. The next strong absorption band at 1736 cm^{-1} was attributed to the stretching of C=O arose from the lipid ester of the liquid crystal. The absorption bands indicated at 1465 and 1375 cm^{-1} were assigned to the C=C stretches of aromatic ring. Sharp and strong peaks of absorption bands observed at 1263 and 1251 cm^{-1} were associated with the C–O aromatic groups. Finger prints for the liquid crystals were characterized by the absorption bands below 1200 cm^{-1}.

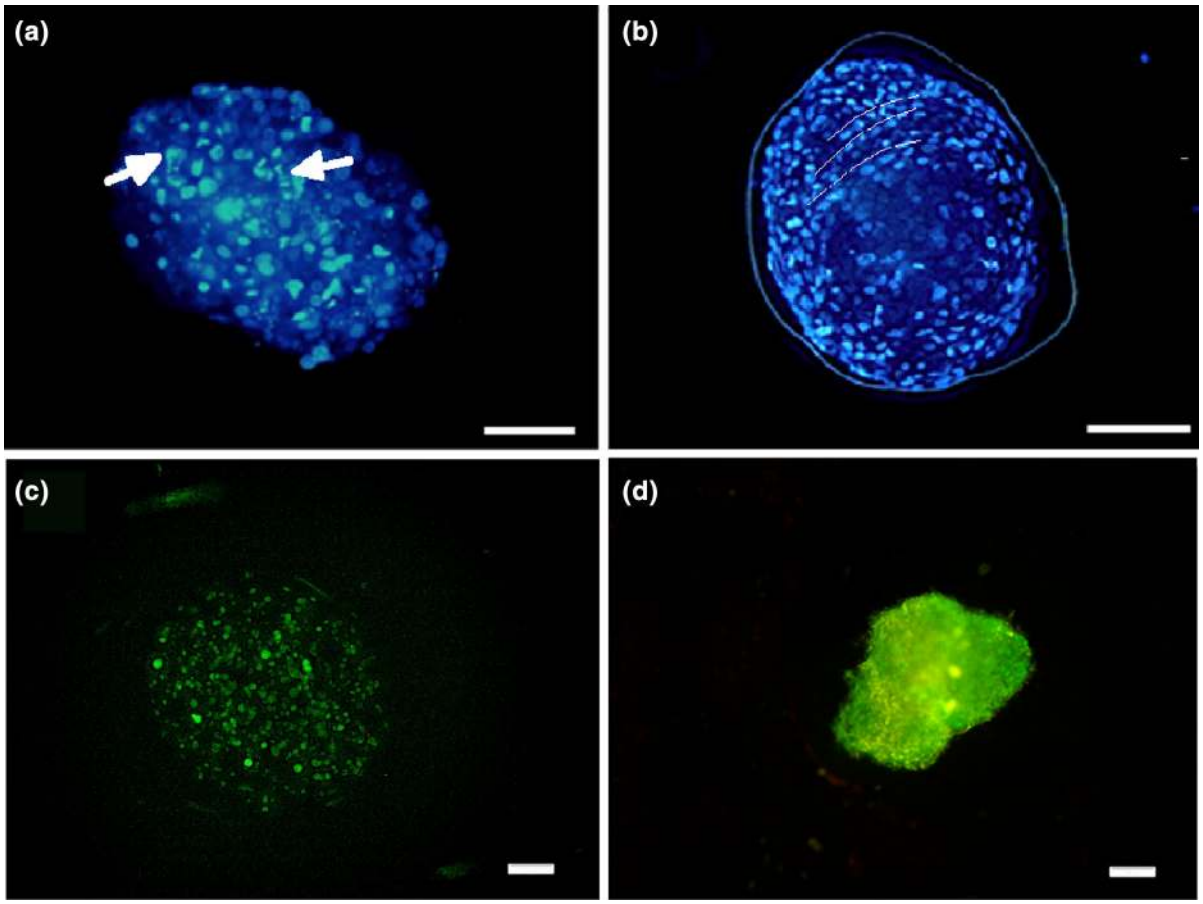

Fig. 6 DAPI stainings of 3D microtissue of cells cultured using **a** alginate microcapsule and **b** liquid crystal substrate (scale bar: 100 μm). The white lines indicate the stratified layers of cells while the white arrows indicate the apoptotic cells. Fluorescence photomicrographs of live and dead cells stainings for microtissues cultured using **c** alginate microencapsulation and **d** liquid crystal substrate (scale bar: 100 μm). The live and dead cells were stained in green (Calcein-AM) and red (Ethidium homodimer), respectively. (Color figure online)

For the microtissues extracted from alginate membrane, the absorption band for C–H groups was determined at 3292 cm^{-1} (Fig. 7b) characterizing the strong phospholipid terminal of CH_3 (Movasaghi et al. 2008). For the calcium alginate microcapsules, the broad band at 3334 cm^{-1} was induced by the C–H hydroxyl groups. However, the dips at 2930 and 2851 cm^{-1} attributed to the C–H stretching of acyl chains (lipids) were found for the microtissues but not for the calcium alginate. The absorption band at 1085 and 1238 cm^{-1} for microtissues was attributed to the asymmetric and symmetric phosphate stretching of PO_2^- associated with nucleic acids and deoxyribonucleic acids, respectively (Malek et al. 2014; Movasaghi et al. 2008). The characteristic bands at 1638 and 1547 cm^{-1} were attributed to the amide I and II of proteins of the microtissues. The peak at 1594.52 cm^{-1} of the calcium alginate spectra was attributed to –OH stretching and the bending vibrations of N–H (amide II band) of proteins. The deformation of C–H, N–H and stretching of C–N in carboxylate of the calcium alginate were identified at 1415 cm^{-1} (Nagpal et al. 2013). For the calcium alginate, the absorption bands at 1030 and 1079 cm^{-1} were assigned to the COH deformation in carbohydrates and C–C stretch of glycogen vibration of polysaccharides, respectively (Malek et al. 2014; Sarker et al. 2013).

Based on the hematoxylin and eosin (H and E) stained histological sections (Fig. 8a, b), microtissues extracted from alginate microcapsules were found with tight packing of cells which is in great contrast to

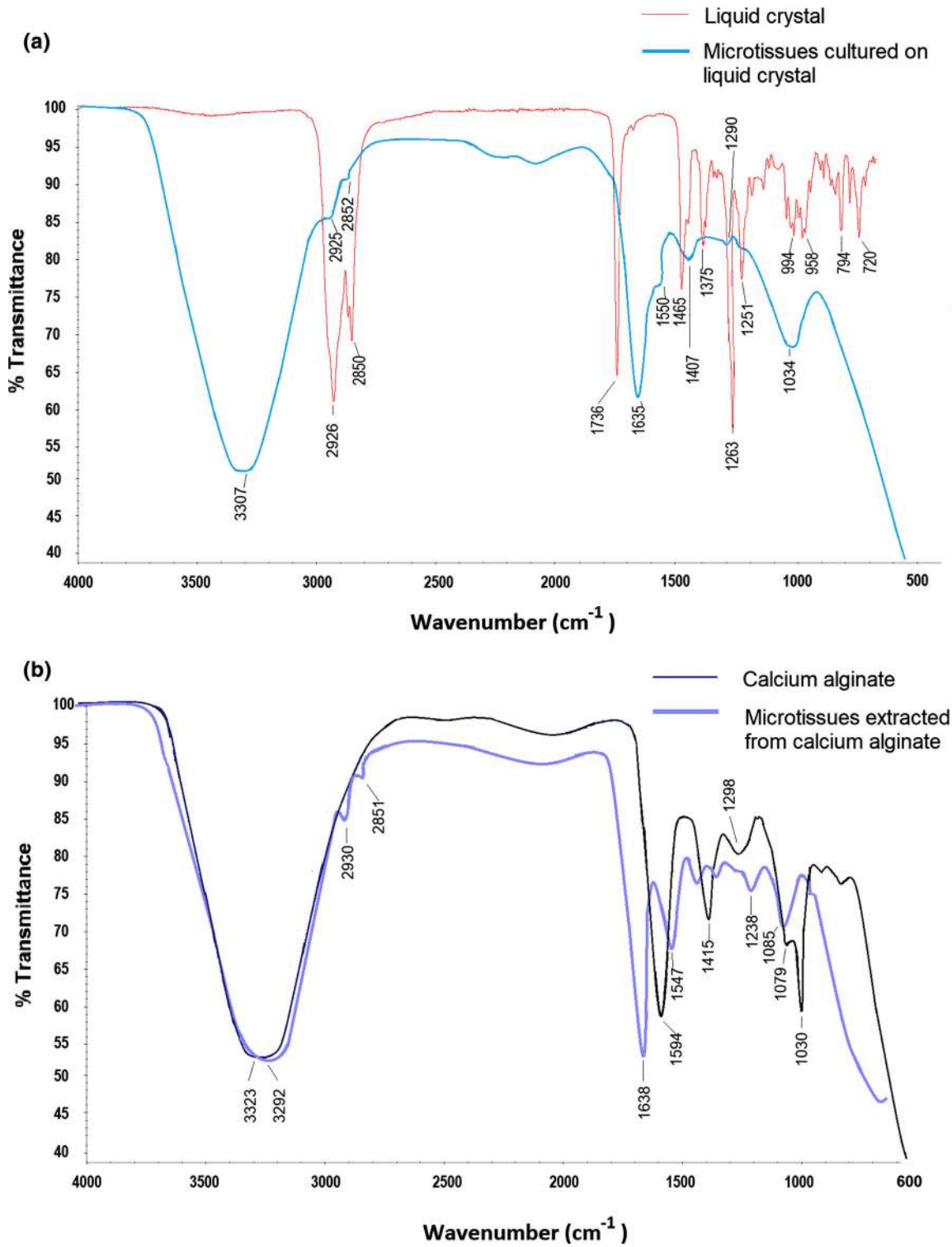

Fig. 7 FTIR spectra of **a** liquid crystal and microtissues extracted from liquid crystal surface, and **b** calcium alginate and microtissues extracted from calcium alginate

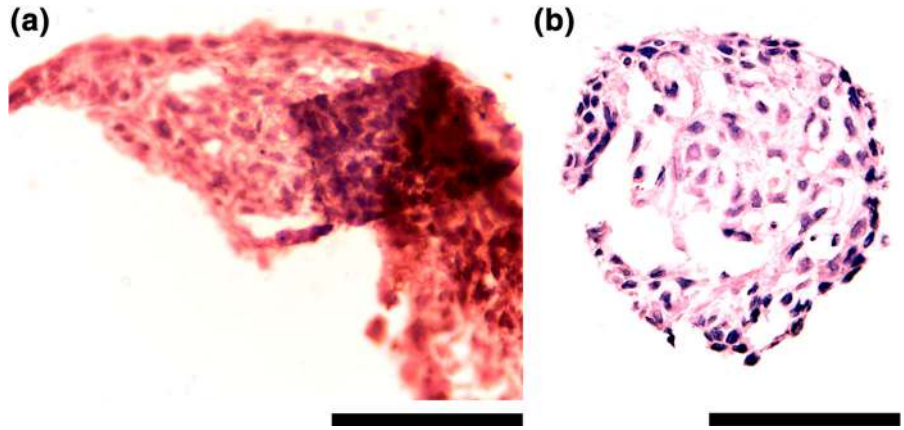

Fig. 8 Histological sectioning and H and E stainings of microtissues cultured using **a** alginate microencapsulation technique and **b** liquid crystal substrate techniques. Pink and purple are the hematoxylin and eosin stains of membrane and nuclei of cells, respectively (scale bar: 100 μm). (Color figure online)

the microtissues formed by self-assembly in liquid crystal culture with more loosely packed cells. With confined spaces in the microcapasules, the gaps between the membranes (pink eosin stains) of cells are small (Fig. 8a). For microtissues formed on the liquid crystal substrate, the cells were indicated with larger spatial distribution of membranes surrounding the nuclei (Fig. 8b) which might be associated with the open space on the liquid crystal culture. For both microtissues (Fig. 8a, b), the cells located at the boundary of the microtissues were closely arranged and shaped according the boundary of the microtissues. It seems that keratinocytes remodeled to maintain the shape of the microtissues. These multilayered cellular structures are found similar to the cell organization in the epidermis layer (Hoath and Leahy 2003).

Discussion

The overall comparison between calcium alginate microencapsulation and liquid crystal substrate based 3D culture techniques are as listed in Table 1. Both techniques are easy to be handled and allow frequent exchange of medium. The exchange of medium may be challenging for other 3D culture techniques such as the hanging drop method (Amy et al. 2012). The intervention of flicker machine generates cellular spheroids of high reproducibility between batches of alginate scaffolds. The spheroid format claimed to be useful in discovering morphological changes in transformed cells (Antoni et al. 2015). Perfectly spherical spheroids may suggest normal cells while distorted structure of microtissues may suggest malignancy of cells (Antoni et al. 2015). In contrast, cells distributed randomly on the liquid crystals produce low quantity of microtissues with highly irregular sizes. The HaCaT cells coalesce into aggregates (keratinospheroids) on the liquid crystal substrate and may undergo epithelial differentiation (James Nelson 2009). The cells grown in capsules took 15 days to form into microspheroids, whereas, the cells seeded on the liquid crystal substrate only took 1 day to form microtissues (Table 1). The microencapsulated cells took longer time to grow into microtissues which could be associated with the suspension culture format (Fig. 2). In the suspension, the cells in microcapsules were floating unsteadily under the buoyant force of culture medium. On the liquid crystal surface, the aggregations of the HaCaT cells were triggered by the mechanical properties and cytocompatibility of the liquid crystal (Soon et al. 2016). Soft and viscoelastic biomaterials with suitable compound mimicking their original physiological organ encouraged the self-regulation of cells into structures that were similar to the native tissues (Discher et al. 2005).

For both cultures, the different growth phases can be identified through the physical measurements. During the lag phase (day 0–5), the cells migrated, assembled and adapted themselves to liquid crystal surface by synthesizing biomolecules for survival

Table 1 Comparison of keratinospheroids cultured using microencapsulation and liquid crystal substrate based 3D culture techniques

Features	Calcium alginate microencapsulation	Liquid crystal substrate
Size	250 ± 31 μm	150 ± 86 μm
Size variability	180–320 μm	50–380 μm
Quantity	350 ± 22	45 ± 15
Reproducibility	High for quantity and size	Low for quantity and size
Morphology	Arbitrary shape after release from alginate membrane	Round or elliptical
Structural formation	Initiates from center core of microspheroids	Self-assembly of cells into aggregates on a planar substrate
Time to form microtissues	~ 15 days	~ 5 days
Stage of growth phases that can be identified	Lag, exponential, stationary and declining phases	Lag, exponential, stationary phases and declining phases
Bio-macromolecules expressed	Amide I/II, phospholipids, nuclei acids	Amide I/II, phospholipids, nuclei acids
Advantages	Ease to replenish new medium	Ease to replenish new medium
	Can produce > 80 pieces of microtissues in single experiment at a cell density of 5×10^7 cells/ml	Allow observation of cell migration
		Can be coated using a cell scrapper
	Size of microcapsules is controllable	Number of microtissues produce < 50 pieces at a cell density of 5×10^6 cells/ml
	Alginate membrane can be applied as immune-isolation layer	3D microtissues contain functional groups of amino acid, nuclei acid and proteins
	3D microtissues contain functional groups of amino acid, nuclei acid and proteins	~ 1 day of culture to form 3D cells
	Microcapsules are easy to handle	
Disadvantages	Need specialised tool or machine to produce controlled size microcapsules	Cells cultured at high density (> $\times 10^6$ cells/ml) formed into sheets
	With limited cell motility	Difficult to control number and size of microtissues developed
	Rupture of alginate membrane	Non-uniformity among microtissues produced
	Required to perform alginate lyase treatment during fluorescence staining	
	~ 15 days of culture to form 3D cells	
Cell viability	~ 100%	~ 100%

(Lodish et al. 2000). The synthesized ECM can be observed in the FE-SEM results (Fig. 5). Once the adaptability to the new environment was established, the cells grew in the exponential phase (day 5–10). During the stationary phase (day 11–25), microtissues in dormant state were formed. The lag, log and stationary phases were identified for microcapsule culture except that the declining phase was not detectable. The main reason is that the alginate microcapsules ruptured after 15 days of immersion in the culture medium leading to the leakage of cells into the culture medium. The monovalent cations produced by the cells could destabilize the calcium alginate microgels over time (Therese Andersen and Dornish 2015). However, for unruptured microcapsules, the cells were found viable up to approximately 30 days of culture. This result showed that the cells encapsulated in the hydrogel-like matrix (size of 250 μm) received sufficient nutrients and gases which allowed them to stay alive after long period of culture (Griffith et al. 2005). The main functions of microencapsulation are to isolate, immobilize and protect the cells in the membrane from their surroundings (Tomaro-Duchesneau et al. 2013). Hence, microencapsulated cells may be suitable for 3D bioprinting applications.

A few smaller and more brightly stained nuclei were observed in the microtissue (Fig. 6a) that could be associated with apoptotic cells. In early apoptosis of cells, there is a degradation of chromatin. This happens simultaneously with the loss of nucleus integrity due to degradation of lamins and reorganization of intranucleus protein matrix (Hendze et al. 1998). These events induce collapse of the nucleus and the aggregation of the heterochromatin appeared as condensed apoptotic chromatin (Hendze et al. 1998). If the cells are dying, the nuclei experiencing apoptosis would appear in smaller and more brightly stained nuclei as indicated in Fig. 6a. However, DAPI staining is an indirect marker of apoptosis. For confirmation of apoptotic cells, live and dead cells stainings can be performed to confirm the presence of apoptotic cells. The live and dead cell stainings for microtissues at dormant phase obtained from liquid crystal and alginate microencapsulation cultures indicated high viability of cells in the 3D microtissues.

Based on the FTIR results, the liquid crystals were determined to have the characteristics of long-chain fatty acids of ester at the absorption bands of 2925 and 2852 cm^{-1}. The cholesteryl ester of the liquid crystal used seemed to have lipids similar to tissue phospholipids (Ziboh and Dreize 1975). Lipid ester is one of the essential materials for building and stabilization of cell membranes for transdermal delivery (Feingold 2007; Norlen et al. 2007). Therefore, liquid crystal contains suitable biochemistry properties in which the cells showed affinity to grow on the substrates (Godugu et al. 2013; Soon et al. 2014). However, the liquid crystal did not influence the biochemistry properties of microtissues because the microtissues were characterized by the absorption bands of typical microtissues as reported previously (Malek et al. 2014) and its FTIR spectra is similar to the FTIR spectra of microtissues produced in alginate microencapsulation (Fig. 7b). The enriched proteins and carboxylated polysaccharides found in the calcium alginate have provided a biocompatible environment for the cells to grow.

Conclusion

The microtissues produced by both techniques differ morphologically and physiologically even though the same cell line was used. Liquid crystal substrate allows natural formation of microspheroids more rapidly than 3D culture based on alginate microcapsule because microcapsules induced physical constraints to cells to form microtissues. Remodeling of cells into microtissues initiated from the center core of microtissues for alginate microencapsulation technique. The microtissues cultured on liquid crystal substrate were built from aggregations of cells on the liquid crystal surface. These spheroids grown in different phases included cells in lag, exponential, stationary and declining phases. The dormant microtissues removed from the alginate microcapsules and liquid crystal cultures were found with homogenous surfaces of tight cell–cell adhesions via ECM proteins. DAPI staining clearly revealed multi-stratified layers of cells organized in microspheroids cultured using the liquid crystal substrate. Contrarily, this well-organized structure was absent in microtissues cultured using alginate microcapsules. In addition, the FTIR spectra of both 3D microtissues indicated the presence of amide, phospholipids and DNA macromolecules. The two techniques presented were able to produce viable microtissues that may be useful for cell biology study over a long period of time. The application in biomedicine is the major consideration in deciding which 3D culture technique to be used.

Acknowledgements The authors are grateful to the research financial support (Science Fund Vot No.: 0201-01-13-SF0104 or S024) awarded by Malaysia Ministry of Science and Technology (MOSTI) and IGSP Grant Vot No. U679 awarded by Universiti Tun Hussein Onn Malaysia. We acknowledge the help of Arina Basyirah Ismail for routine cell sub-culture.

Author's contribution CFS produced the conception of the paper and prepared the manuscript of the paper. KST designed and fabricated the flicker machine. SCW performed the microencapsulation of 3D cells and quantification of microtissues. CFS conducted the 3D cell culture and staining experiments of the microtissues. NN performed the FE-SEM imaging of the microtissues. MKA conducted the FTIR experiments and NS analyzed the FTIR results. FS helped to analyze and interpret the cells staining results. MY synthesized and prepared the liquid crystals. SA/LS prepared the samples for the histological sectioning.

Compliance with ethical standards

Conflict of interest None of the authors have any competing interest in the manuscript.

Ethics approval Cell lines were used in the experiments. Not applicable.

References

Amy YH, Yi-Chung T, Xianggui Qu, Lalit RP, Kenneth JP, Shuichi T (2012) 384 hanging drop arrays give excellent Z-factors and allow versatile formation of co-culture spheroids. Biotechnol Bioeng 109:1293–1304. https://doi.org/10.1002/bit.24399

Antoni D, Burckel H, Josset E, Noel G (2015) Three-dimensional cell culture: a breakthrough in vivo. Int Mol Sci 16:5517–5527. https://doi.org/10.3390/ijms16035517

Discher D, Janmey P, Y-l Wang (2005) Tissue cells feel and respond to the stiffness of their substrate. Science 310:1139–1143. https://doi.org/10.1126/science.1116995

Edmondson R, Broglie JJ, Adcock AF, Yang L (2014) Three-dimensional cell culture systems and their applications in drug discovery and cell-based biosensors. Assay Drug Dev Technol 12:207–218. https://doi.org/10.1089/adt.2014.573

Fang Y, Elgen RM (2017) Three-dimensional cell cultures in drug discovery and development. SLAS Discov 1:1–17. https://doi.org/10.1177/2472555217696795

Feingold K (2007) The role of epidermal lipids in cutaneous permeability barrier homeostasis. J Lipid Res 48:2531–2546. https://doi.org/10.1194/jlr.R700013-JLR200

Godugu C, Patel AR, Desai U, Andey T, Sams A, Singh M (2013) AlgiMatrix^{TM} based 3D cell culture system as an in vitro tumor model for anticancer studies. PLoS ONE 8:e53708. https://doi.org/10.1371/journal.pone.0053708

Griffith CK, Miller C, Sainson RC, Calvert JW, Jeon NL, Hughes CC, George SC (2005) Diffusion limits of an in vitro thick prevascularized tissue. Tissue Eng 11:257–266. https://doi.org/10.1089/ten.2005.11.257

Hendze M, Nishioka W, Raymond Y, Allis C, Bazett-Jones D, TnJ PH (1998) Chromatin condensation is not associated with apoptosis. J Biol Chem 273:24470–24478. https://doi.org/10.1074/jbc.273.38.24470

Hirschhaeuser F, Menne H, Dittfeld C, West J, Mueller-Klieser W, Kunz-Schughart L (2010) Multicellular tumor spheroids: an underestimated tool is catching up again. J Biotechnol 148:3–15. https://doi.org/10.1016/j.jbiotec.2010.01.012

Hoath SB, Leahy DG (2003) The organization of human epidermis: functional epidermal units and phi proportionality. J Invest Dermatol 121:1440–1446. https://doi.org/10.1046/j.1523-1747.2003.12606.x

Hongisto V, Jernstrom S, Fey V (2013) High-throughput 3D screening reveals differences in drug sensitivities between culture models of JIMT1 breast cancer cells. PLoS ONE 8:e77232. https://doi.org/10.1371/journal.pone.0077232

Jackson M, Mantsch H (1995) The use and misuse of FTIR spectroscopy in the determination of protein structure. Crit Rev Biochem Mol Biol 30:95–120. https://doi.org/10.3109/10409239509085140

James Nelson W (2009) Remodeling epithelial cell organization: transitions between front–rear and apical–basal polarity. Cold Spring Harb Perspect Biol 1:a000513. https://doi.org/10.1101/cshperspect.a000513

Kundu AK, Khatiwala CB, Putnam AJ (2009) Extracellular matrix remodeling, integrin expression, and downstream signaling pathways influence the osteogenic differentiation of mesenchymal stem cells on poly(lactide-co-glycolide) substrates. Tissue Eng Part A 15:273–283. https://doi.org/10.1089/ten.tea.2008.0055

Kunz-Schughart L, Freyer J, Hofstaedter F, Ebner R (2014) The use of 3-D cultures for high throughput screening: the multicellular spheroid model. J Biomol Screen 9:273–285. https://doi.org/10.1177/1087057104265040

Lodish H, Berk A, Zipursky SL, Matsudaira P, Baltimore D, Darnell J (2000) Molecular cell biology, 6th edn. Freeman & Co Ltd, W.H

Luca A, Mersch S, Deenen R (2013) Impact of the 3D microenvironment on phenotype, gene expression, and EGFR inhibition of colorectal cancer cell lines. PLoS ONE 8:e59689. https://doi.org/10.1371/journal.pone.0059689

Malek K, Wood BR, Bambery KR (2014) FTIR imaging of tissues: techniques and methods of analysis. In: Malgorzata B (ed) Optical spectroscopy and computation methods in biology and medicine, vol 14. Springer, Dordrecht, pp 419–474

Movasaghi Z, Rehman S, Rehman Iu (2008) Fourier transform infrared (FTIR) spectroscopy of biological tissues. Appl Spectrosc Rev 43:134–179. https://doi.org/10.1080/05704920701829043

Nagpal M, Singh SK, Mishra D (2013) Synthesis characterization and in vitro drug release from acrylamide and sodium alginate based superporous hydrogel devices. Int J Pharm Investig 3:131–140. https://doi.org/10.4103/2230-973X.119215

Nirmalanandhan VS, Duren A, Hendricks P, Vielhauer G, Sittampalam GS (2010) Activity of anticancer agents in a three-dimensional cell culture model. Assay Drug Dev Technol 8:581–590. https://doi.org/10.1089/adt.2010.0276

Norlen L, Plasencia G, Simonsen A, Descouts P (2007) Human stratum corneum lipid organization as observed by atomic force microscopy on langmuir–blodgett films. J Struct Biol 158:386–400. https://doi.org/10.1016/j.jsb.2006.12.006

Sarker B, Papageorgiou DG, Silva R, Boccaccini AR (2013) Fabrication of alginate-gelatin crosslinked hydrogel microcapsules and evaluation of the microstructure and physico-chemical properties. J Mater Chem B 2:1470–1482. https://doi.org/10.1039/C3TB21509A

Soon CF, Youseffi M, Berends RF, Blagden N, Denyer MC (2013) Development of a novel liquid crystal based cell traction force transducer system. Biosens Bioelectron 39:14–20. https://doi.org/10.1016/j.bios.2012.06.032

Soon CF et al (2014) Biophysical characteristics of cells cultured on cholesteryl ester liquid crystals. Micron 56:73–79. https://doi.org/10.1016/j.micron.2013.10.011

Soon CF et al (2016) A scaffoldless technique for self-generation of three-dimensional keratinospheroids on liquid crystal surfaces. Biotech Histochem 91:283–295. https://doi.org/10.3109/10520295.2016

Souza GR et al (2010) Three-dimensional tissue culture based on magnetic cell levitation. Nat Nanotechnol 5:291–296. https://doi.org/10.1038/nnano.2010.23

Therese Andersen PA-E, Dornish M (2015) Review 3D cell culture in alginate hydrogels. Microarrays 4:133–161. https://doi.org/10.3390/microarrays4020133

Thoma C, Stroebel S, Rösch N, Calpe B, Krek W, Kelm J (2013) A high-throughput-compatible 3D microtissue co-culture system for phenotypic RNAi screening applications.

J Biomol Screen 18:1330–1337. https://doi.org/10.1177/1087057113499071

Tomaro-Duchesneau C, Saha S, Malhotra M, Kahouli I, Prakash S (2013) Microencapsulation for the therapeutic delivery of drugs, live mammalian and bacterial cells, and other biopharmaceutics: current status and future directions. J Pharm 2013:1–17. https://doi.org/10.1155/2013/103527

Vantangoli MM, Madnick SJ, Huse SM, Weston P, Boekelheide K (2015) MCF-7 human breast cancer cells form differentiated microtissues in Scaffold-free hydrogels. PLoS ONE 10:e0135426. https://doi.org/10.1371/journal.pone.0135426

Wang S, Wong Po Foo C, Warrier A, Poo MM, Heilshorn SC, Zhang X (2009) Gradient lithography of engineered proteins to fabricate 2D and 3D cell culture microenvironments. Biomed Microdev 11:1127–1134. https://doi.org/10.1007/s10544-009-9329-1

Wong SC, Soon CF, Leong WY, Tee KS (2016) Flicking technique for microencapsulation of cells in calcium alginate leading to the microtissue formation. J Microencapsul 33:162–171. https://doi.org/10.3109/02652048.2016.1142017

Yamada KM, Cukierman E (2007) Modeling tissue morphogenesis and cancer in 3D. Cell 130:601–610. https://doi.org/10.1016/j.cell.2007.08.006

Ziboh V, Dreize M (1975) Biosynthesis and hydrolysis of cholesteryl esters by rat skin subcellular fractions. Biochem J 152:281–289. https://doi.org/10.1042/bj1520281